Synthesis, Photophysical, and Electroluminescent Properties of Arylenevinylenes-*co*-pyrrolenevinylenes Derived from Divinylaryl Bridged Bispyrroles

Anand K. Biswas,[†] Ashish Ashish,[||] Awnish K. Tripathi,[‡] Yashowanta N. Mohapatra,*[,†,‡,||] and Ayyappanpillai Ajayaghosh*[,†,||,§]

Materials Science Programme, Indian Institute of Technology, Kanpur, India-208016, Department of Physics, Indian Institute of Technology, Kanpur, India-208016, Photosciences and Photonics Group, Regional Research Laboratory, CSIR, Trivandrum, 695 019, India, and Samtel Centre for Display Technologies, Indian Institute of Technology, Kanpur, India-208016

Received January 16, 2007; Revised Manuscript Received February 16, 2007

ABSTRACT: Synthesis, characterization, and photophysical properties of four different π-conjugated oligomers containing alternate arylenevinylene and pyrrolenevinylene repeat units are reported. The optoelectronic properties are traced from the molecules to oligomers and to thin films and single layer electroluminescent (EL) devices. These oligomers exhibited strong absorption and emission corresponding to $\pi-\pi^*$ transitions which vary with electronic nature of the aryl moieties. The band gaps of these oligomers are in the range 1.84−2.04 eV and they emit in the orange to red region. The photoluminescence (PL) spectra of the oligomers **P1**−**P4** in solution and film state are significantly different from each other. The time-resolved fluorescence decay in dichloromethane solution showed a fast decay profile for the anthracene-bridged oligomer and a relatively slow decay for benzene-bridged oligomer. Polymer light emitting diodes (PLEDs) with single active layer of oligomers with the configuration ITO/PEDOT:PSS/oligomer/Ca/Al exhibited low turn on voltages and yellow to deep red emission. Though the anthracene-bridged oligomer did not show any detectable PL in the film state, a weak electroluminescence (EL) emission around 730 nm was observed.

Introduction

The discovery of electroluminescence in poly(*p*-phenylenevinylene)s (PPVs) has generated considerable interest in the design of a variety of new polymers and oligomers.[1−3] As a result, the past decade has witnessed the development of a plethora of strategies in the design of new materials and their use as active components in polymer light emitting diodes (PLEDs), thin film transistors (TFTs), and photovoltaic devices.[4−8] Organic semiconducting polymers have the inherent advantages of easy structural modification and solution processability. From the chemistry viewpoint, a crucial aspect of the design strategy is the choice of the proper monomer with suitable electron donating or withdrawing groups on the polymer backbone in order to facilitate the modulation of the HOMO−LUMO gap, thereby allowing the molecule to emit, virtually at any wavelength in the visible region. The selection of monomers with suitable side chains greatly influences the intermolecular interactions and the electronic properties. These requirements have prompted chemists to the design of a variety of copolymers which allowed the control and tuning of the optoelectronic properties.[4,9−13] From the device viewpoint, the semiconducting polymers should have good thermal and chemical stability and should lead to high electroluminescent (EL) efficiency at low turn on voltage. The commonly used aromatic heterocycles for the synthesis of π-conjugated polymers for optoelectronic applications are thiophene, bithiophene, benzothiazole, carbazole, and phenothiazine derivatives.[14−21] Polypyrroles have been shown to exhibit high redox stability, high conductivity, and better electrochromic properties. In addition, structurally modified pyrroles with aromatic bridging groups have been shown to influence the oxidation potentials for electropolymerization.[22−23] However, pyrroles and its derivatives have not received proper attention to the synthesis of electroluminescent polymers though there is a report on a solution processable 2,5-pyrrolenevinylene as a low band gap conducting polymer.[24]

Table 1. Yield (%), M_w, M_n, PDI (M_w/M_n), and T_d (°C) of Oligomers (P1−P4)

oligomers	yield (%)	M_w[a]	M_n[a]	PDI (M_w/M_n)	T_d[b] (°C)
P1	52	5586	2527	2.2	413
P2	68	30 583	11 558	2.7	388
P3	73	14 200	3491	4.1	326
P4	53	1586	1167	1.4	324

[a] Determined by GPC, relative to polystyrene standards. [b] TGA was done under nitrogen atmosphere at a heating rate of 10 °C/min.

The band gap of linear polyaromatic conjugated systems are determined mainly by contributions from the energy related to bond length alteration, the mean deviation from planarity, the aromatic resonance energy of the cycle, the inductive or mesomeric effects of the substituents, and the intermolecular or interchain interactions in the solid state.[25] The changes in such properties need to be studied when the monomers are converted to oligomers, in addition to their suitability as thin films, and ultimately as used in a device setting. The logic of changes occurring at each stage of this hierarchy from monomers to device applications need to be understood. For strategies of design, it is essential to understand the role of a variety of bridging groups and correlate their influence upon optoelectronic properties.

* Corresponding authors. (A.A.) Telephone: (+91) 471 515 306. Fax: (+91) 471 491 712. E-mail: aajayaghosh@rediffmail.com.(Y.N.M.) Telephone: (+91) 512 259 6621. Fax: (+91) 512 259 6620. E-mail: ynm@iitk.ac.in.

[†] Materials Science Programme, Indian Institute of Technology.

[‡] Department of Physics, Indian Institute of Technology.

[§] Photosciences and Photonics Group, Regional Research Laboratory, CSIR.

[||] Samtel Centre for Display Technologies, Indian Institute of Technology.

10.1021/ma070116g CCC: $37.00
Published on Web 03/24/2007

Scheme 1. Syntheses of Bispyrroles (B1−B4) and the Corresponding Arylenevinylene-*co*-pyrrolenevinylene Oligomers (P1-P4)

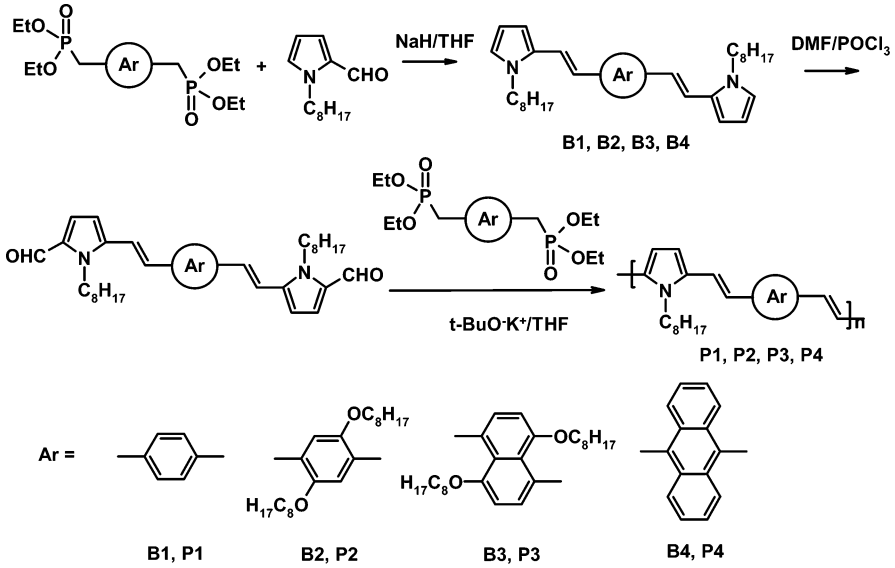

During the past few years we have been interested in the design of arylbridged bispyrroles, which can be used as a monomer for the design of a variety of π-conjugated materials. In this context, we have reported the synthesis and electropolymerization of several bispyrroles containing aromatic bridging units.[26] They are also useful to the design of functional dye based low band gap systems.[27] Herein, we report the use of these fluorescent building blocks for the synthesis of arylenevinylene-*co*-pyrrolenevinylene oligomers. Detailed studies on characterization, photophysical, and electroluminescent properties are reported. We trace transformations from molecules (bispyrroles) to oligomers, and from thin films to devices to reveal the comparative logic of inclusion of bridging groups and, hence, their role in tailoring the optoelectronic properties of materials derived from bispyrroles.

Results and Discussion

Synthesis and Characterization. The bispyrroles **B1**−**B4** were synthesized as per reported procedures.[26] Synthesis of the oligomers **P1**−**P4** involves the Vilsmeyer formylation of bispyrroles **B1**−**B4**, followed by Wittig−Horner−Emmons olefination[28] using the required bisphosphonates in the presence of *t*-BuO$^-$K$^+$ in THF (Scheme 1). Dark colored products were obtained by reprecipitation with CH_2Cl_2/ MeOH followed by Soxhlet extraction with methanol. The yield of oligomers ranged from 52 to 73%. The number-average molecular weight (M_n) and the weight-average molecular weight (M_w) of the oligomers, as determined by gel permeation chromatography (GPC) using THF mobile phase and polystyrene standards, ranged from 1167 to 11558 (M_n) and from 1586 to 30583 (M_w), respectively with polydispersity indices ranging from 1.4 to 4.1, indicating the products are mainly oligomers. In Table 1, the yield, molecular weight, polydispersity, and thermal stability of the oligomers are presented. The thermogravimertic analysis (TGA) of the oligomers was carried out in nitrogen atmosphere at a heating rate of 10 °C/min. The oligomers exhibit an onset of degradation between 324 and 413 °C. ^{1}H NMR spectra of oligomers showed the required resonance peaks of the aromatic and vinylic protons (δ 8.3−6.5 ppm), −NCH_2 and −OCH_2 protons (δ ∼4.0 ppm), and the aliphatic protons (δ 2.00−0.8 ppm). In addition, ^{1}H NMR spectra of oligomers also showed weak resonance peaks at δ 9.4 (terminal C*H*O), and 4.4 ppm (OCH_2 and NCH_2) corresponding to terminal groups. The all-trans conformations of the oligomers were confirmed from their FT−IR spectral analysis, which revealed the absorption corresponding to the C−H out-of-plane vibrational mode of the *trans*-vinylic group at 950 cm^{-1}.

Absorbance and Photoluminescence Spectra. Bispyrrole Monomers (B1—B4) in Solution. The normalized absorption and emission spectra of **B1**−**B4** in dichloromethane (DCM, 10^{-5} M) are shown in Figure 1, and the data are summarized in Table 2. They showed structureless absorbance maxima in the range 375−429 nm that are typical of their $\pi-\pi^*$ transitions. A considerable shift in $\pi-\pi^*$ transitions is noticed with change of the bridging units. The 1,4-dioctyloxybenzene substituted bispyrrole **B2** showed a red shift of 13 nm when compared to the absorption maximum of the unsubstituted benzene derivative **B1** in DCM, due to the electron-donating effect of bisoctyloxy

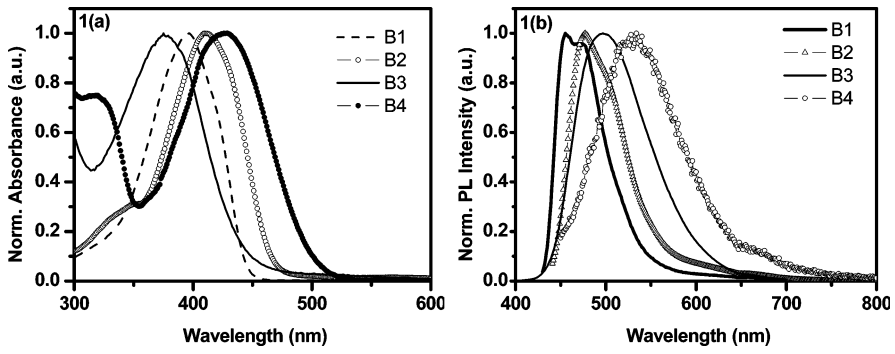

Figure 1. (a) UV−vis absorption and (b) photoluminescence (PL) spectra of bispyrroles in dichloromethane solution (10^{-5} M).

Table 2. Optical Properties of Bispyrroles (B1−B4) in DCM Solutions (10^{-5} M)

	λ_{max} (nm)		
bispyrrole	UV-vis abs[a]	PL emission	τ (ns) TATS lifetime[a,b]
B1	397	455 (474)	0.98 [100%]
B2	410	477 (500)	1.44 [100%]
B3	375	497	3.13 [100%]
B4	429	534	0.197 [83.3%], 1.25 [16.7%]

[a] Absorption, emission, and lifetimes were determined in dichloromethane solution. [b] Lifetimes were determined by fitting time analyzed transient spectroscopy (TATS) spectra of corresponding time correlated single photon counting (TCSPC) photoluminescence decay.

groups. On the other hand, a 22 nm blue shift can be noticed in the absorption maximum of the naphthalene-bridged bispyrrole **B3** when compared to that of the bispyrrole **B1**, indicating a less planar conformation of the π-backbone, due to the steric requirement of the 4,8-bisoctyloxynaphthalene groups. However, the anthracene bridged derivative **B4** showed maximum red-shifted absorption spectra with the absorption maximum around 429 nm.

The PL emission spectrum of the unsubstituted divinylbenzene-bridged-bispyrrole **B1** is significantly different from those of **B2**−**B4**. The former shows a structured emission with two maxima at 455 and 474 nm. The bisoctyloxybenzene-bridged compound **B2** showed an emission maximum at 477 nm with a shoulder around 500 nm, whereas the bisoctyloxynaphthalene-bridged derivative **B3** and anthracene derivative **B4** showed broad emission spectra with maxima around 497 and 534 nm in DCM. It is interesting to note that the naphthalene (**B3**) and anthracene (**B4**) derivatives showed large Stokes shift of 122 and 105 nm respectively, when compared to the other two derivatives which showed Stokes shift of 58 and 67 nm for **B1** and **B2** respectively.

The difference between **B1** and **B2** lies in the presence of the electron donating side chains of the latter, which reduces both the energy of absorption and emission. The trend of lowering peak energy of absorption and emission simultaneously continues with the introduction of anthracene as the bridging unit. The trend in the series **B1**, **B2**, and **B4** (with the exception of **B3**) clearly shows increased delocalization, either due to electron-donating side chains or the aromatic group which in turn leads to progressive decrease in the energy gap. We summarize these conclusions in a simplified configuration coordinate diagram as shown in Figure 2. We kept the total energy corresponding to LUMO as the reference and adjusted the mean coordinate and curvature of HOMO level of the different compounds (bispyrroles) so as to account the experimental values of emission and absorption in the process. However, naphthalene-bridged compound does not belong to this trend and shows increase in energy of absorption, though emission energy shifts as expected. This can be understood as a relative shift of the total energy curves corresponding to the HOMO level along the coordinate axis in a configuration coordinate diagram. That would induce higher absorption energy and lower PL emission energy with **B1** and **B2** serving as reference. Clearly, naphthalene-bridged unit along with the alkoxy side chains leads to distortion of the molecule, in the form of deviation in planarity, which can be represented as a shift in the configuration coordinate and increase in the curvature. The comparative diagram implies significant qualitative features: (i) the effect of side chains as in going from **B1** to **B2** is to cause decrease in energy alone; (ii) addition of a cyclic unit laterally changes the stiffness constants; (iii) cyclic units in the presence of the side chain causes significant distortion affecting both coordinate and curvature significantly.

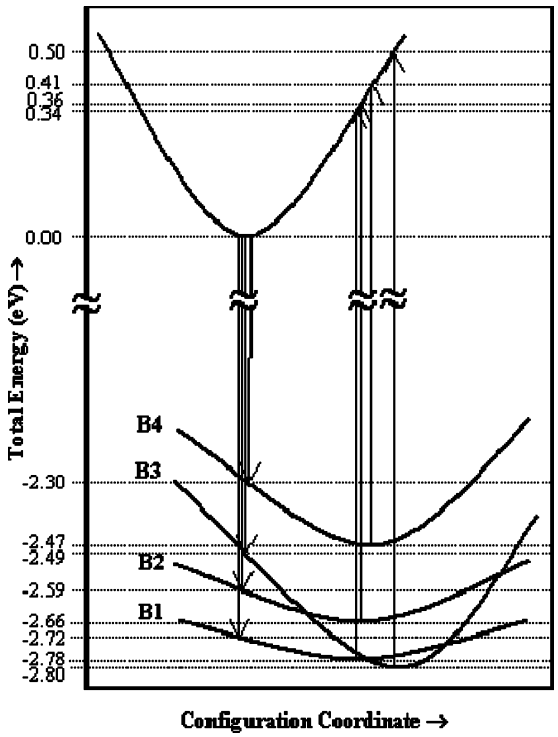

Figure 2. Schematic configuration coordinate diagram for the purpose of comparison. Total energy corresponding to LUMO was taken as reference. Energies corresponding to band gaps (HOMO−LUMO) were calculated from onsets of absorption spectra of bispyrroles in solution.

Oligomers (P1—P4) in Solution. The normalized absorption and emission spectra of oligomers **P1**−**P4** in DCM are shown in Figure 3, and the photophysical data are summarized in Table 3. **P1**−**P4** show structureless absorption spectra with their maxima in the range of 440−538 nm and are typical of $\pi-\pi^*$ transitions. The oligomer **P2** showed a red shift of 36 nm when compared to the absorption maximum of **P1** indicating electron-donating effect of bisoctyloxy groups as observed in the corresponding bispyrrole. There may be some contribution to red shift of spectra due to molecular weight differences of **P1** and **P2**. The absorption maxima of **P1** and **P2** exhibited large red shifts of 105 and 128 nm, respectively, compared to those for their corresponding bispyrroles **B1** and **B2**. These large red shifts are attributed to the enhanced effective conjugation length of the oligomers. The absorption maxima of oligomers **P3** and **P4** are ca. 60 nm blue-shifted compared to **P1** indicating that the degree of conjugation is lesser in these systems. The PL emission spectra of the oligomers **P1** and **P2** are structured with their maxima around 587 and 623 nm along with shoulders around 626 and 670 nm, respectively. The emission spectra of **P3** and **P4** are broad and structureless which are blue-shifted by approximately 28 nm when compared to **P1**. Both **P3** and **P4** showed large Stokes shifts of nearly 120 nm. Comparative configuration coordinate diagrams can be constructed along the lines of Figure 2 for the case of oligomers as well. Note that the large out-of-plane distortion in naphthalene-bridged molecule seems to reduce significantly when the molecule is extended to oligomer chain. The lateral addition of cyclic units then cause little changes as seen in the case of **P3** and **P4**, where the emission and absorption bands are virtually the same except for difference in broadness with the anthracene bridge causing larger variations.

Table 3. Photophysical and Device Properties of Oligomers (P1−P4)

	λ_{max} (nm)				τ (ns)		
oligomer	UV−vis abs (solution)[a]	PL emission (solution)[a]	UV−vis abs (thin film)[c]	PL emission (thin film)[c]	TATS lifetime (solution)[a,b]	λ_{max} (nm) EL emission[d]	CIE coordinate
P1	502	587 (626)	487	620 (665)	1.12 [100%]	620 (670)	(0.66, 0.33)
P2	538	623 (670)	558	655 (695)	0.473 [96.7%], 1.73 [3.3%]	650(700)	(0.71, 0.29)
P3	441	559	434	574 (664)	0.455 [53.6%], 1.45 [46.4%]	600	(0.53, 0.46)
P4	440	560	454		0.151 [64.6%], 1.04 [20.74%], 3.59 [14.7%]	730	(0.68, 0.32)

[a] Absorption, emission, and lifetimes were determined in dichloromethane solution. [b] Lifetimes were determined by fitting TATS spectra of corresponding TCSPC photoluminescence decay. [c] Absorption and emission spectra were measured on quartz substrates by spin-casting 10 mg/mL solution of oligomers in toluene and dried under vacuum. [d] Devices were fabricated with the following configuration: ITO/PEDOT:PSS/oligomer/Ca/Al.

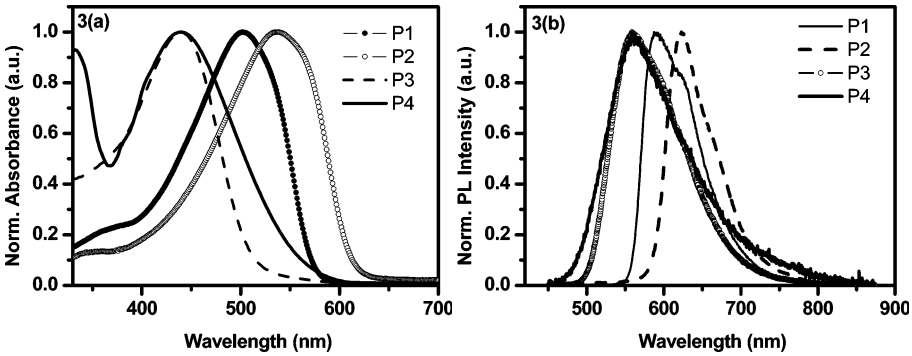

Figure 3. (a) UV−vis absorption spectra and (b) photoluminescence (PL) spectra of oligomers in dichloromethane solution (10^{-5} M).

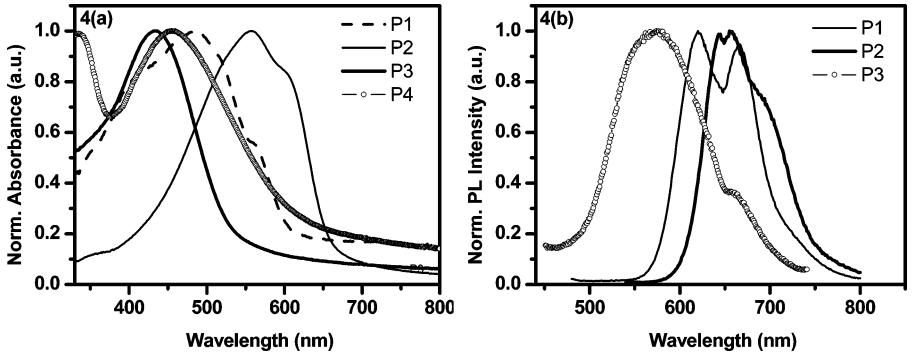

Figure 4. (a) UV−vis absorption spectra and (b) photoluminescence (PL) spectra of oligomers on quartz substrates. Films were prepared by spin-casting 10 mg/mL solution of oligomers in toluene and dried under vacuum.

Thin Films of Oligomers (P1—P4). Thin film absorption and PL emission spectra of the oligomers **P1**−**P4** on quartz substrates are shown in Figure 4, and the data are given in Table 3. The maxima of absorption spectra are centered around 434−558 nm. The oligomer **P1** shows a structured absorption with maximum at 487 nm and shoulders around 410 and 560 nm. The oligomer **P2** absorption maximum is red-shifted to 36 nm when compared to **P1** with its maximum at 558 nm and shoulder at 600 nm. The oligomers **P3** and **P4** exhibit broad and structureless spectra and are blue-shifted when compared to **P1** and **P2**. The onsets of the thin film absorption spectra were used to determine the band gap of the oligomers. The calculated band gaps for oligomers **P1**−**P4** are in the range of 1.84−2.04 eV and are shown in a schematic band diagram in Figure 7. The PL emission spectra are structured in the case of **P1** and **P2**. For example, **P1** has two maxima at 620 and 665 nm while the emission spectrum of **P2** has a maximum at 655 nm and shoulder at 695 nm. The emission spectrum of **P3** is broad and blue-shifted compared to both **P1** and **P2** with maximum at 574 nm and a shoulder around 664 nm. Surprisingly, the film of **P4** was practically nonemissive, indicating very strong self-quenching in the solid state.

A comparison of trends in the spectral properties of bispyrroles and oligomers from solution to thin films is best summarized as follows:

(i) The trends in the case of benzene bridged bispyrroles (**B1** and **B2**) and oligomers (**P1** and **P2**) are as expected both in solution and thin films. The side chains lead to longer conjugation, lesser degree of sharpness in phonon-related features, and larger red-shifted spectra due to solid-state effect.

(ii) The nonplanarity of the naphthalene bridged bispyrrole (**B3**) seems to be arrested in its oligomer (**P3**) form as can be deduced from the relative changes in emission and absorption energies. Both absorption and emission energies of oligomer (**P3**) increases compared to benzene derivative (**P1**), while absorption energy increases and emission energy decreases in the case of **B3** compared to the benzene bridged bispyrrole (**B1**).

(iii) The optical properties of naphthalene and anthracene bridged oligomers (**P3** and **P4**) are dominated by the presence of the lateral aromatic units shortening the effective conjugation along the length of the chain compared to benzene derivatives (**P1** and **P2**). However, only comparison of the absorption and PL spectra of oligomer **P3** and **P4** exhibited minor differences in width (fwhm) indicating that the influence of dialkoxy side

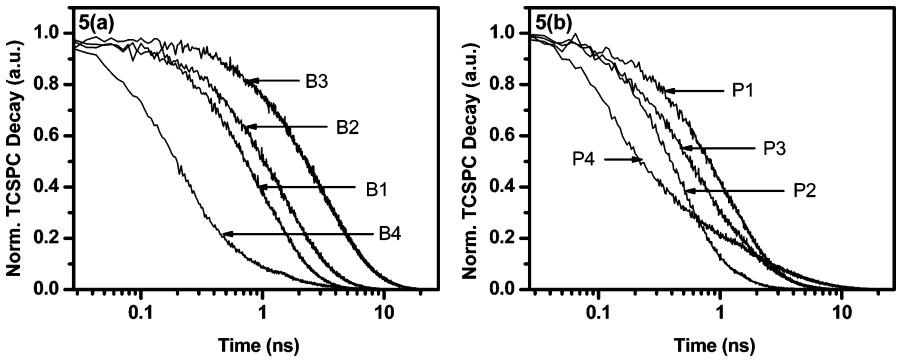

Figure 5. Time correlated single photon counting (TCSPC) for (a) bispyrrole monomers **B1**−**B4** and (b) oligomers **P1**−**P4**. The decay profiles were recorded in dichloromethane solution (10^{-5} M). For better visualization, the intensity is plotted against logarithm of time.

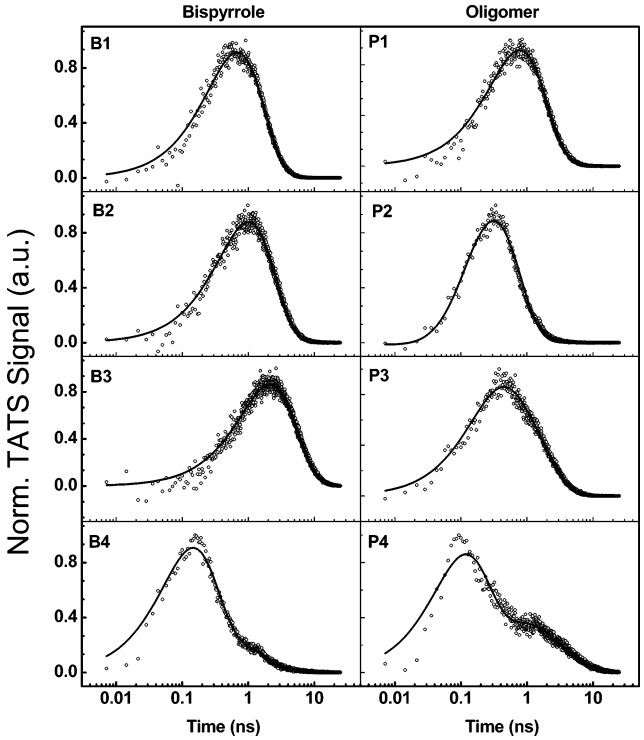

Figure 6. Time analyzed transient spectroscopy (TATS) spectra (circles) of bispyrrole monomers (**B1**−**B4**) and oligomers (**P1**−**P4**) and their corresponding fittings (lines). Time constants obtained from fittings are given in Tables 2 and 3 for bispyrroles and oligomers, respectively. Note the spectroscopic character of the curves highlighting the utility of such analysis.

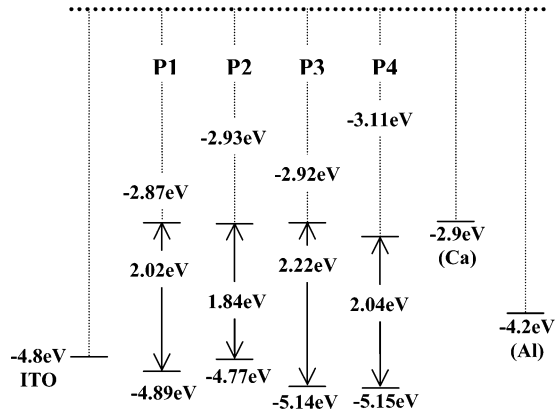

Figure 7. Schematic band diagram of oligomers. Band gaps were calculated from onsets of absorption spectra. HOMO levels were calculated from onsets of cyclic voltammetry curves of the thin films of oligomers cast on Pt electrode. The LUMO levels were calculated from corresponding band gaps and HOMO values.

chains in **P3** and the additional lateral aromatic groups in **P4** are small in tuning the optical properties

(iv) In thin films, the naphthalene and anthracene bridged oligomers (**P3** and **P4**) are likely to have increased stacking due to $\pi-\pi$ interaction. This is borne out by the nearly complete cessation of PL in the case of **P4** and severely constrained conjugation in the case of **P3** with broad structureless and low wavelength emission.

TCSPC Lifetime Measurements and TATS Analysis of Bispyrrole Monomers and Oligomers in Dilute Solution. Time correlated single photon counting (TCSPC) lifetime measurements of the bispyrrole monomers and oligomers are shown in Figure 5. For better visualization, the decay profiles are plotted differently from conventional method, by plotting the time in logarithmic scale against the normalized PL intensity. TCSPC decay profiles for both bispyrrole monomers and the corresponding oligomers show marked influence of varying bridging groups. Naphthalene-bridged bispyrroles show a very slow decay while anthracene-bridged bispyrrole decay very fast. Benzene and bisoctyloxybenzene-bridged decay profiles are in between. Among oligomers, **P1** shows the slowest decay profile whereas **P4** shows very fast decay.

Often, multiple exponential fitting is nonunique and leads to mistaken conclusions unless sufficient care is taken in checking their validity and significance. Therefore, we resort to time analyzed transient spectroscopy (TATS) which is a more reliable method of analyzing decay curves using spectroscopic analysis within the time domain.[29] In this technique, the TATS signal is defined as

$$S(t) = [I(t) - I(t + \gamma t)]$$

where γ is an experimentally selectable constant and $I(t)$ is the PL intensity transient. In the extreme limit of γ tending to zero the signal becomes a derivative of the signal in log time. For a perfect exponential this signal has a definite peak line shape, and the time constant can be obtained from the time at which the peak occurs. The presence of multiple peaks or distribution of time constants may be more easily and reliably inferred from such an analysis. The TATS spectra of bispyrrole monomers (**B1**−**B4**) and oligomers (**P1**−**P4**) and their corresponding fitting are shown in Figure 6. Time constants so obtained for bispyrroles and oligomers are tabulated in Table 2 and Table 3, respectively.

As discussed earlier, the radiative decay time of **B3** and **B4** in solution is very different from **B1** and **B2**. While nonplanarity of **B3** molecule leads to a long-lived singlet, the presence of an extra ring in the anthracene bridge seems to open up fast nonradiative paths of decay, leading to multiple exponentials.

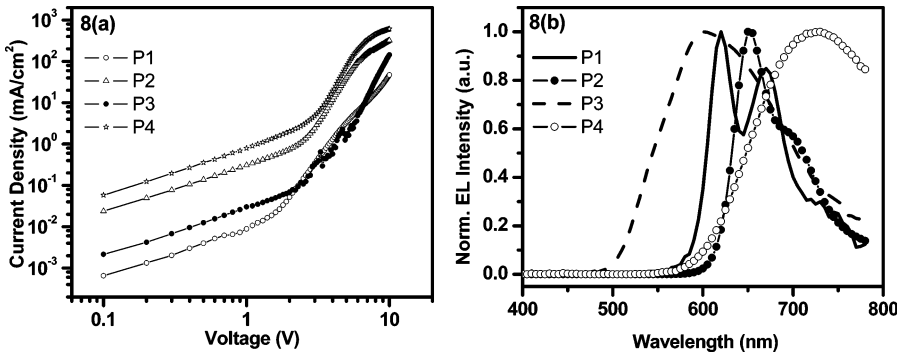

Figure 8. (a) Log−log plot of current density−voltage (J-V) characteristics; and (b) EL emission spectra of devices: ITO/PEDOT:PSS/oligomer/Ca/Al.

In the oligomer form, hindrance to nonplanarity causes the decay of **P2** and **P3** to go through similar pathways. The presence of an anthracene bridge provides a fast decay path both in monomer **B4** and in oligomer **P4.**

Electrochemical Properties of Oligomers. Cyclic voltammetry (CV) was employed to investigate the redox behavior of the oligomers and to estimate the HOMO (highest occupied molecular orbital) levels. The characteristic data were measured for a thin film cast on a platinum electrode with active disk area of 2.0 mm^2 at a scan rate of 100 mV/s. Ag/AgCl was used as reference electrode and Pt wire as counter electrode. Tetrabutyl ammonium perchlorate was used as a supporting electrolyte. Oligomers were found to be electrochemically inert in the reduction region and exhibited only irreversible oxidation onsets except in the case of **P4** where both onset oxidation and reduction potentials were observed. The onset oxidation potentials of **P1**−**P4** were determined to be 0.49, 0.37, 0.74, and 0.75 V, respectively which were used to determine the highest occupied molecular orbitals (HOMO) of the oligomers using empirical formula: $E_{(HOMO)} = -(E_{ox} + 4.40)$ (eV).[30] The LUMO levels were determined using the equation: $E_{(LUMO)} = E_{(HOMO)} - E_g$, where E_g (band gaps) were calculated from thin film absorption onsets. The HOMO, LUMO and band gap of oligomers as determined are shown in a schematic band diagram in Figure 7. The LUMO levels of **P1**−**P3** are not much affected due to a change of aromatic units in the main chain except in the case of **P4** where the LUMO level is slightly lower. The HOMO level of **P2** is slightly higher when compared to **P1** and that of **P3** and **P4** are lower when compared to both **P1** and **P2**. The CV curve of the oligomer **P4** shows the reduction onset at −0.89 V, and the LUMO level calculated was found to be −3.51 eV. Therefore, the band gap of the oligomer thus determined was found to be only 1.64 eV, which is very different from 2.04 eV as calculated from absorption band-edge, indicating the existence of large relaxation of oligomer **P4** in solid-state configuration coordinate. It is to be noted that the HOMO and LUMO levels of the whole series of compounds are conveniently close to ITO and Ca electrodes respectively, making it convenient for device applications.

Electroluminescence (EL) Spectra and Current Density—Voltage (*J*—*V*) Characteristics. Single active layer PLED devices were fabricated using thin films of the oligomers with ITO/PEDOT:PSS serving as hole injection electrode, and Ca/Al for electron injection in a conventional configuration as ITO/PEDOT:PSS/oligomer/Ca/Al. The intention was not to optimize the performance of PLEDs but to continue the comparative study of the optoelectronic properties of the oligomers in a device environment. Electroluminescence (EL) spectra and current density−voltage (*J*−*V*) characteristics are shown in Figure 8. EL spectra of oligomers are similar to their thin film PL spectra. EL emission of **P1** shows two discernible peaks around 620 and 670 nm whereas **P2** based devices emit with a maximum at 650 nm with a shoulder around 700 nm. **P1** and **P2** devices were found to emit in the red region with their CIE coordinates being (0.66, 0.33) and (0.71, 0.29), respectively. The **P3** shows a broad and structureless EL emission and emit in the yellow-orange region with CIE coordinate (0.53, 0.46). Though we could not observe any detectable thin film PL in oligomer **P4** but a red-shifted EL emission could be seen with maximum around 730 nm with CIE coordinate (0.68, 0.32). The current density−voltage characteristics of devices show typical diode behavior with the turn on voltage of devices varying from 4.0 V − 8.0 V, when all conditions of processing are kept the same without regard to optimization of parameters such as thickness for each individual case. As expected of typical PLEDs, the characteristics show transition from trap charge limited current to space charge limited current at higher voltages. The varying resistances of the layer control the threshold voltage and the corresponding current below it.

The absence of PL and the observation of red-shifted EL for anthracene-bridged **P4** oligomer is a significant pointer to the difference in mechanism of luminescence in the two conditions. Clearly, excitations with the above band gap energy give rise to singlet excitations, which get quenched due to the $\pi-\pi$ interaction of stacked oligomers in the thin film. However, when oppositely charged polarons are injected from the two electrodes, the possibility of forming interchain species due to randomness of the charged species increases greatly. The red emission in **P4** devices therefore can be attributed to long-range interchain singlet excitons observed only during electroluminescence. The ranges of compounds discussed are good candidates for orange-red emission. The mobilities measured (not reported here) from EL transient experiments are comparable or better than MEH−PPV devices. The overlap integral for anthracene-bridged oligomer is large, pointing toward its possible use for TFT applications as well. The mobility related electronic properties would be reported elsewhere.

Conclusions

The aryl bridged bispyrroles **B1**−**B4** and the corresponding oligomers **P1**−**P4** containing alternate arylenevinylene and pyrrolenevinylene repeating units exhibited interesting opto-electronic behavior in solution and solid state. Optical properties of the monomers and oligomers are influenced greatly by the varying electronic nature of the bridging groups. The configuration coordinate diagram could be conveniently used to understand the effect of bridging units on the optical properties of molecules. The effect of electron-donating side chains is to cause decrease in total energy alone in a configuration coordinate diagram while the addition of cyclic units laterally or incorpora-

tion of fused polyaromatic groups such as naphthalene and anthracene as bridging unit causes significant distortion affecting both coordinate and curvature significantly. The oligomers were luminescent both in solution as well in thin film state except for anthracene-bridged derivative possibly due to greater $\pi-\pi$ interchain interactions. The solution absorption and emission spectra of naphthalene and anthracene bispyrrole derivatives are quite different but corresponding oligomers spectra are quite similar suggesting the overall effect on optical properties in both cases are similar. It can be also inferred that the overall decrease in effective conjugation in anthracenevinylene bridged oligomer is due to nonplanarity similar to 4,8-bisoctyloxy-1,5-naphthlenevinylene bridged oligomers. Lifetime measurements and TATS analysis of PL decay showed the significant influence of different bridging groups. The anthracene derivative shows a fast radiative behavior both in monomer and oligomer form while other derivatives show relatively slow decay profiles. The calculated HOMO and LUMO levels of all oligomers are conveniently close to ITO and Ca for easy injection of charge carriers in a conventional device configuration and found to be electroluminescent in yellow to deep red region with low turn on voltages. Absence of PL in thin film state of anthracene bridged oligomer and simultaneous EL emission suggests the formation of long-range interchain excitons. In summary, we have shown the empirical trends in the role of bridging groups in the bispyrroles and the corresponding oligomers on their optoelectronic properties. The insights so obtained can be gainfully utilized in the design of conjugated oligomers and polymers for specific applications.

Experimental Section

General Data. All chemicals purchased from Aldrich Chemicals Co. were used as received unless otherwise stated. Other chemicals used were purified using standard procedures. The melting points were measured by using a capillary melting point apparatus and were uncorrected. ^{1}H and ^{13}C NMR were recorded on Jeol JNM-LA400 FT−NMR system. FT−IR of samples was recorded on Bruker Vertex 70 FT−IR spectrometer. FAB mass spectra were recorded on a JEOL SX 102/DA-6000 mass spectrometer/data system using argon/xenon (6 kV, 10 mA) as the FAB gas. The accelerating voltage was 10 kV and the spectra were recorded at room temperature. *m*-Nitrobenzyl alcohol (NBA) was used as the matrix. Gel permeation chromatography was performed using THF as eluent and polystyrene as standard on a Waters GPC system. Themogravimetric analyses were performed on TA thermal analyzer under nitrogen atmosphere at a heating rate of 10 °C/min. UV−vis absorption spectra were measured using a Perkin-Elmer Lambda 40 UV/vis spectrometer. Photoluminescence (PL) data were recorded on a Jobin Yvon Horiba Fluorolog-3 system (absorption maxima was used as excitation wavelength) for bispyrrole solution and oligomer thin films. Oligomer solution PL was obtained through optical fiber using Ocean Optics SD2000 spectrometer (excitation wavelength was 442 nm). Dilute solutions of monomers and oligomers were prepared in dichloromethane (DCM). Thin films were prepared on quartz substrates by spin-coating oligomer solution of concentration 10 mg/mL in toluene. Time correlated single photon counting (TCSPC) measurements were performed in DCM using IBH 5000U fluorescence lifetime system. A violet LED of wavelength 403 nm was used as excitation source and emission was collected at PL maxima. The electrochemical measurements were performed on a Epsilon CV voltametric analyzer using tetrabutylammonium perchlorate (TBAP) (0.1 M) in acetonitrile as electrolyte at a scan rate of 100 mV/s. Pt wire and Ag/AgCl electrode were used as the counter and reference electrode, respectively. For this purpose, oligomers drop-casted from 5 to 10 μL of DCM solution (concentration 10−12 mg/mL) onto a Pt disk were used as working electrodes (BAS MF-2013) with an active area of 2.0 mm^2.

General Procedure for Preparation of Bisformyl Derivatives of Bispyrroles. The Vilsmeyer formylation reaction of bispyrroles gave the respective bisformyl derivatives in 51−68% yield. To a solution of bispyrrole (0.5 mmol) in 1,2-dichlorobenzene (25 mL) at 0 °C, Vilsmeyer reagent which was prepared by slow addition of $POCl_3$ (0.15 mL, 1.4 mmol) into a flask containing DMF (0.33 mL, 5.8 mmol) at 0 °C, was added. The mixture was stirred at 0 °C for 3 h and then poured into crushed ice. The solution was heated on a water bath and then neutralized with sodium acetate. The mixture was again heated on a water bath for 10−15 min with stirring until clear separation of water and organic layer appears and then extracted with dichloromethane. Removal of the solvent gave the crude products, which were further purified by column chromatography using ethyl acetate/ hexane (5:95 or 10:90) to give the pure products.

(*E*,*E*)-1,4-Bis[2-(1-octyl-5-formylpyrrol-2-yl)vinyl]benzene. Yield: 58%. Mp: 108−110 °C. ^{1}H NMR ($CDCl_3$, 400 MHz): δ 9.41 (s, 2H), 7.43 (s, 4H), 7.06 (d, J = 16.12 Hz, 2H), 6.93 (d, J = 16.12 Hz, 2H), 6.86 (d, J = 2.2 Hz, 2H), 6.53 (d, J = 4.4 Hz, 2H), 4.40 (t, J = 7.56 Hz, 4H), 1.69−1.65 (m, 4H), 1.27−1.18 (m, 20H), 0.79 (t, J = 7.08 Hz, 6H) ppm. ^{13}C NMR ($CDCl_3$, 100 MHz): δ 178.59, 140.74, 136.62, 132.17, 131.99, 127.02, 125.21, 115.40, 108.07, 45.02, 31.78, 31.43, 29.22, 29.18, 26.58, 22.61, 14.08 ppm. FT−IR: (KBr): ν_{max} 2927, 2853, 2813, 2771, 1644, 1509, 1463, 1394, 1289, 1210, 1143, 1042, 957, 870, 798, 764 cm^{-1}. MS (FAB, *m*/*z*): 540 (M^+).

(*E*,*E*)-1,4-Bis[2-(1-octyl-5-formylpyrrol-2-yl)vinyl]-2,5-dioctyloxybenzene. Yield: 68%. Mp: 84−86 °C. ^{1}H NMR ($CDCl_3$, 400 MHz): δ 9.47 (s, 2H), 7.38 (d, J = 16.4 Hz, 2H), 7.26 (d, J = 14.4 Hz, 2H), 7.04 (s, 2H), 6.96 (d, J = 3.6 Hz, 2H), 6.26 (d, J = 4.0 Hz, 2H), 4.48 (t, J = 8.0, 6.8 Hz, 4H), 4.07 (t, J = 6.4 Hz, 4H), 1.97−1.50 (m, 8H), 1.32−1.25 (m, 40H), 0.87−0.85 (m, 12H) ppm. ^{13}C NMR ($CDCl_3$, 100 MHz): δ 178.3, 151.3, 141.9, 132.0, 128.5, 126.4, 125.4, 116.6, 111.8, 108.0, 69.2, 45.1, 31.8, 31.5, 29.3, 26.7, 26.2, 22.6, 14.1 ppm. FT−IR (KBr): ν_{max} 2925, 2853, 2363, 1655, 1508, 1469, 1404, 1233, 1202, 1034, 954, 783, cm^{-1}. MS (FAB, *m*/*z*): 796 (M^+).

(*E*,*E*)-1,5-Bis[2-(1-octyl-5-formylpyrrol-2-yl)vinyl]-4,8-dioctyloxynaphthalene. Yield: 54%. Mp: 58−56 °C. ^{1}H NMR ($CDCl_3$, 400 MHz): δ 9.37 (s, 2H), 8.22 (d, J = 15.36 Hz, 2H), 7.35 (d, J = 8.04, 2H), 6.86 (d, J = 4.16 Hz, 2H), 6.83 (d, J = 8.04, 2H), 6.47 (d, J = 4.88, 2H), 6.44 (d, J = 16.08 Hz, 2H), 4.39 (t, J = 6.84, 4H), 3.99 (t, J = 6.12 Hz, 4H), 1.77−1.60 (m, 12H), 1.16−1.08 (m, 36H), 0.79 (t, J = 6.84 Hz, 12H) ppm. ^{13}C NMR ($CDCl_3$, 100 MHz): δ 177.92, 156.92, 142.42, 138.94, 131.41, 128.17, 126.96, 113.08, 107.16, 69.20, 44.97, 31.84, 31.78, 31.43, 29.55, 29.38, 29.27, 29.18, 26.63, 26.49, 22.60, 14.06 ppm. FT−IR (KBr): ν_{max} 2924, 2854, 1653, 1523, 1525, 1467, 1399, 1367, 1312, 1277, 1211, 1140, 1072, 1040, 954, 775 cm^{-1}. MS (FAB, *m*/*z*): 846 (M^+).

(*E*,*E*)-9,10-Bis[2-(1-octyl-5-formylpyrrol-2-yl)vinyl]anthracene. Yield: 51%. Mp: 72−74 °C. ^{1}H NMR ($CDCl_3$, 400 MHz): δ 9.49 (s, 2H), 8.27 (dd, J = 3.64, 2.44 Hz, 4H), 7.92 (d, J = 16.08 Hz, 2H), 7.42 (dd, J = 3.16, 3.2 Hz, 4H), 6.97 (d, J = 4.16 Hz, 2H), 6.81 (d, J = 15.6 Hz, 2H), 6.80 (d, J = 4.36 Hz, 2H), 4.35 (t, J = 7.32 Hz, 4H), 1.70−1.58 (m, 8H), 1.21−1.11 (m, 16H), 0.74 (t, J = 6.6 Hz, 6H) ppm. ^{13}C NMR ($CDCl_3$, 100 MHz): δ 178.9, 140.5, 132.2, 132.2, 129.4, 129.1, 126.1, 125.7, 125.1, 124.8, 108.0, 45.2, 31.7, 29.2, 29.1, 26.6, 22.5, 14.0 ppm. FT−IR (KBr) ν_{max}: 2924, 2854, 2369, 1655, 1521, 1466, 1405, 1367, 1261, 1209, 1095, 1037, 961, 794 cm^{-1}. MS (FAB, *m*/*z*): 640 (M^+).

General Procedure for Preparation of Oligomers. To ice−water cold (~10 °C) solutions of the formyl derivative of bispyrroles (0.5 mmol) and the respective bisphosphonate esters (0.5 mmol) in 25 mL of dry THF was added 1.0 mL of *t*-BuO^-K^+ (1.0 M in THF solution, Aldrich) dropwise. Soon after the addition of the base, the greenish color of the solution changed into reddish brown. The reaction mixture was stirred overnight at room temperature. THF was evaporated and methanol was added to precipitate the dark colored product. The oligomers were further purified by

reprecipitation with CH_2Cl_2/MeOH followed by Soxhlet extraction with methanol. The yields of the oligomers ranged from 52 to 73%.

P1. Yield: 52%. ^{1}H NMR (CD_2Cl_2, 400 MHz): δ 9.4 (s, *trace, terminal* −C*H*O), 7.4 (m, 4H, *vinylic*), 6.9 (m, 4H, *aromatic*), 6.6 (s, 2H, *pyrrole*), 4.4 (*trace terminal* −NCH_2−), 4.0 (m, 2H, −NCH_2−), 1.6−0.8 (m, 15H, −(CH_2)$_6$CH_3) ppm. FT−IR(KBr): ν_{max} 3019, 2852, 1652, 1613, 1502, 1464, 1502, 1464, 1403, 1260, 1093, 1028, 946 cm^{-1}.

P2. Yield: 68%. ^{1}H NMR (CD_2Cl_2, 400 MHz): δ 7.2 (s, 4H, *vinylic*), 7.0 (s, 2H, *aromatic*), 6.6 (s, 2H, *pyrrole*), 4.0 (m 6H, −NCH_2− and −OCH_2−), 1.9−1.3 (m, 36H, −(CH_2)$_6$− × 3), 0.89 (m, 9H, −CH_3 × 3) ppm. FT−IR (KBr): ν_{max} 2924, 2855, 1610, 1461, 1412 1205, 1034, 950 cm^{-1}.

P3. Yield: 73%. ^{1}H NMR (CD_2Cl_2, 400 MHz) δ 9.4 (s, *trace, terminal* −C*H*O), 8.1 (m, 2H, *aromatic*), 7.4 (m, 2H, *vinylic*), 6.9 (m, 2H, *aromatic*), 6.5 (m, 4H, *pyrrole and vinylic*), 4.4 (*trace terminal* −NCH_2− and −OCH_2−), 4.0 (m, 6H, −NCH_2 and −OCH_2−), 1.91−0.85 (m, 45H, −(CH_2)$_6$CH_3 × 3) ppm. FT−IR (KBr) ν_{max}: 2923, 2854, 1653, 1579, 1519, 1463, 1373, 1312, 1272, 1205, 1035, 950 cm^{-1}.

P4: Yield: 53%. ^{1}H NMR (CD_2Cl_2, 400 MHz) δ 9.5 (s, *trace terminal* C*H*O), 8.5−7.8 (m, 6H, *aromatic and vinylic*), 7.5 (m, 6H, *aromatic and vinylic*), 6.9 (m, 2H, *pyrrole*), 4.4 (s, 2H, −NCH_2−), 4.0 (s, *trace*), 1.7−1.2 (m, 12H, −(CH_2)$_6$−), 0.82 (s, 3H, −CH_3) ppm. FT−IR (KBr) ν_{max}: 2922, 2852, 1653, 1464, 1043, 1367, 1028, 954 cm^{-1}.

Device Fabrication and Characterization. The devices were fabricated using commercially available ITO coated glass substrates. The ITO substrates were patterned by usual photolithographic processing. The substrates were cleaned with RCA-I solution. A 15 min ozone treatment was done to remove any residual organic matter. A thin layer of polyethylene dioxythiophene/polystyrene-sulfonate (PEDOT:PSS), purchased from Bayer Corporation, was spin-coated at 1800 rpm and baked at 120 °C for 2 h under vacuum. The emissive layer was then spin-coated at 1000 rpm from oligomer solutions of conc. 10−12 mg/mL in chlorobenzene and filtered through 10.0 μm filter (Millipore Co.), and then dried under vacuum at 120 °C for 2 h. A ∼20 nm thick Ca cathode was deposited through a mask in a vacuum evaporator at a pressure of ∼10^{-6} mbar. An additional layer of Al (∼400 nm) was then evaporated on top of Ca layer under the same condition yielding an active area of 10 mm^2. Thin glass substrates, coated with epoxy, were used to seal devices. Epoxy was cured under UV light for 20 min. Current−voltage (I−V) characteristics were measured using Keithley 236 source measure unit. EL spectra were recorded using a Minolta spectroradiometer in the range of 380−780 nm.

Acknowledgment. We thank the Department of Science and Technology (DST), Government of India, and Samtel Group of Industries, New Delhi, India, for financial support. A Ramanna Fellowship by DST to A.A. is gratefully acknowledged. This is contribution No. RRLT-PPG 244.

References and Notes

(1) Burroughes, J. H.; Bradley, D. D. C.; Brown, A. R.; Marks, R. N.; Mackay, K.; Friend, R. H.; Burns, P. L.; Holmes, A. B. *Nature (London)* **1990**, *347*, 539.

(2) (a) Gustafsson, G.; Cao, Y.; Treacy, G. M.; Klavetter, F.; Colaneri, N.; Heeger, A. J. *Nature (London)* **1992**, *357*, 477. (b) Friend, R. H.; Gymer, R. W.; Holmes, A. B.; Burroughes, J. H.; Marks, R. N.; Taliani, C.; Bradley, D. D. C.; Dos Santos, D. A.; Brédas, J. L.; Logdlund, M.; Salaneck, W. R. *Nature (London)* **1999**, *397*, 121.

(3) Gigli, G.; Barbarella, G.; Favaretto, L.; Cacialli, F.; Cingolani, R. *Appl. Phys. Lett.* **1999**, *75*, 439.

(4) (a) Kraft, A.; Grimsdale, A. C.; Holmes, A. B. *Angew. Chem., Int. Ed.* **1998**, *37*, 402. (b) Shim, H. -K.; Jin, J.-I. *Adv. Polym. Sci.* **2002**, *158*, 193.

(5) (a) Halik, M.; Klauk, H.; Zschieschang, U.; Kriem, T.; Schmid, G.; Radlik, W.; Wussow, K. *Appl. Phys. Lett.* **2002**, *81*, 289. (b) Kawase, T.; Shimoda, T.; Newsome, C.; Sirringhaus, H.; Friend, R. H. *Thin Solid Films* **2003**, *438*−*439*, 279. (c) Park, J.; Park, S. Y.; Shim, S.-O.; Kang, H.; Lee, H. H. *Appl. Phys. Lett.* **2004**, *85*, 3283.

(6) (a) Brabec, C. J.; Sariciftci, N. S.; Hummelen, J. C. *Adv. Funct. Mater.* **2001**, *11*, 15. (b) Dhanabalan, A.; van Duren, J. K. J.; van Hal, P. A.; van Dongen, J. L. J.; Janssen, R. A. J. *Adv. Funct. Mater.* **2001**, *11*, 255. (c) Brabec, C. J.; Winder, C.; Sariciftci, N. S.; Hummelen, J. C.; Dhanabalan, A.; van Hal, P. A.; Janssen, R. A. J. *Adv. Funct. Mater.* **2002**, *12*, 709. (d) Tsai, M.-H.; Lin, H.-W.; Su, H.-C.; Ke, T.- H.; Wu, C.; Fang, F.-C.; Liao, Y.-L.; Wong, K.-T.; Wu, C.-I. *Adv. Mater.* **2006**, *18*, 1216.

(7) Wienk, M. M.; Kroon, J. M.; Verhees, W. J. H.; Knol, J.; Hummelen, J. C.; van Hal, P. A.; Janssen, R. A. J. *Angew. Chem., Int. Ed.* **2003**, *42*, 3371.

(8) Yang, R.; Tian, R.; Yan, J.; Zhang, Y.; Yang, J.; Hou, Q.; Yang, W.; Zhang, C.; Cao, Y. *Macromolecules* **2005**, *38*, 244.

(9) (a) Kang, I.-N.; Hwang, D. H.; Shim, H.-K.; Zyung, T.; Kim, J.-J. *Macromolecules* **1996**, *29*, 165. (b) Ahn, T.; Ko, S.-W.; Lee, J.; Shim, H.-K. *Macromolecules* **2002**, *35*, 3495. (c) Liao, L.; Pang, Y.; Ding, L.; Karasz, F. E. *J. Polym. Sci., Polym. Chem.* **2003**, *41*, 3149. (d) Yamamoto, T.; Arai, M.; Kokubo, H.; Sasaki, S. *Macromolecules* **2003**, *36*, 7986.

(10) (a) Ranger, M.; Rondeau, D.; Leclerc, M. *Macromolecules* **1997**, *30*, 7686. (b) Cho, N. S.; Hwang, D.-H.; Lee, J.-I.; Jung, B.-J.; Shim, H.-K. *Macromolecules* **2002**, *35*, 1224. (b) Jacob, J.; Zhang, J.; Grimsdale, A. C.; Müllen, K.; Gaal, M.; List, E. J. W. *Macromolecules* **2003**, *36*, 8240.

(11) (a) Beaupré, S.; Leclerc. M. *Adv. Funct. Mater.* **2002**, *12*, 192. (b) Lim, E.; Jung, B.-J.; Shim, H.-K. *Macromolecules* **2003**, *36*, 4288. (c) Kong, X.; Kulkarni, A. P.; Jenekhe, S. A. *Macromolecules* **2003**, *36*, 8992. (d) Cho, N. S.; Hwang, D.-H.; Jung, B.-J.; Oh, J.; Chu, H.-Y.; Shim, H.-K. *Synth. Met.* **2004**, *143*, 277. (e) Lee, J.; Cho, H.-J.; Jung, B.-J.; Cho, N. S.; Shim, H.-K. *Macromolecules* **2004**, *37*, 8523.

(12) (a) Klärner, G.; Davey, M. H.; Chen, W.-D.; Miller, R. D. *Adv. Mater.* **1998**, *10*, 993. (b) Miteva, T.; Meisel, A.; Knoll, W.; Notherfer, H. G.; Scherf, U.; Müller, D. C.; Meerholz, K.; Yasuda, A.; Neher, D. *Adv. Mater.* **2001**, *13*, 565.

(13) (a) Ahn, T.; Shim, H.-K. *Macromol. Chem. Phys.* **2001**, *202*, 3180. (b) Hou, Q.; Xu, Y.; Yang, W.; Yuan, M.; Peng, J.; Cao, Y. *J. Mater. Chem.* **2002**, *12*, 2887. (c) Niu, Y.-H.; Hou, Q.; Cao, Y. *Appl. Phys. Lett.* **2003**, *82*, 2163. (d) Ego, C.; Marsitzky, D.; Becker, S.; Zhang, J.; Grimsdale, A. C.; Müllen, K.; Mackenzie, J. D.; Silva, C.; Friend, R. H. *J. Am. Soc. Chem.* **2003**, *125*, 437. (e) Hwang, D.-H.; Lee, J.-D.; Kang, J.-M.; Lee, S.; Lee, C.-H.; Jin, S.-H. *J. Mater. Chem.* **2003**, *13*, 1540.

(14) (a) Pei, J.; Yu, W.-L.; Huang, W.; Heeger, A. J. *Macromolecules* **2000**, *33*, 2462. (b) Lai, R. Y.; Fabrizio, E. F.; Lu, L.; Jenekhe, S. A.; Bard, A. J. *J. Am. Chem. Soc.* **2001**, *123*, 9112. (c) Shen, Z.; Strauss, J.; Daub, J. *Chem. Commun.* **2002**, 460.

(15) (a) Alam, M. M.; Tonzola, C. J.; Jenekhe, S. A. *Macromolecules* **2003**, *36*, 6577. (b) Lai, R. Y.; Kong, X.; Jenekhe, S. A.; Bard, A. J. *J. Am. Chem. Soc.* **2003**, *125*, 12631. (c) Fungo, F.; Jenekhe, S. A.; Bard, A. J. *Chem. Mater.* **2003**, *15*, 1264.

(16) (a) Sun, D.; Rosokha, S. V.; Kochi, J. K. *J. Am. Chem. Soc.* **2004**, *126*, 1388. (b) Hou, Q.; Zhou, Q.; Zhang, Y.; Yang, W.; Yang, R.; Cao, Y. *Macromolecules* **2004**, *37*, 6299. (c) Cho, N. S.; Hwang, D.-H.; Jung, B.-J.; Lim, E.; Lee, J.; Shim, H.-K. *Macromolecules* **2004**, *37*, 5265. (d) Fang, Q.; Jiang, B.; Xu, B.; Wang, W.; Yu, F.; Wu, X. *Macromol. Rapid Commun.* **2004**, *25*, 1429.

(17) (a) Yeh, H.-C.; Yeh, S.-J.; Chen, C.-T. *Chem. Commun.* **2003**, 2632. (b) Yeh, H.-C.; Chan, L.-H.; Wu, W.-C.; Chen, C.-T. *J. Mater. Chem.* **2004**, *14*, 1293. (c) Jenekhe, S. A.; Lu, L.; Alam, M. M. *Macromolecules* **2001**, *34*, 7315. (d) Hwang, D.-H.; Kim, S.-K.; Park, M.-J.; Lee, J.-H.; Koo, B.-W.; Kang, I.-N.; Kim, S.-H.; Zyung, T. *Chem. Mater.* **2004**, *16*, 1298.

(18) (a) Yang, J.; Jiang, C.; Zhang, Y.; Yang, R.; Yang, W.; Hou, Q.; Cao, Y. *Macromolecules* **2004**, *37*, 1211. (b) Peng, Q.; Lu, Z.-Y.; Huang, Y.; Xie, M.-G.; Han, S.-H.; Peng, J-B.; Cao, Y. *Macromolecules* **2004**, *37*, 260.

(19) (a) Lim, E.; Jung, B.-J.; Lee, J.; Shim, H. K.; Lee, J.-I.; Yang, Y. S.; Do, L.-M. *Macromolecules* **2005**, *38*, 4531. (b) Yang, R.; Tian, R.; Yan, J.; Zhang, Y.; Yang, J.; Hou, Q.; Yang, W.; Zhang, C.; Cao, Y. *Macromolecules* **2005**, *38*, 244.

(20) Perepichka, I. F.; Perepichka, D. F.; Meng, H.; Wudl, F. *Adv. Mater.* **2005**, *17*, 2281.

(21) (a) Cho, N. S.; Park, J.-H.; Lee, S.-K.; Lee, J.; Shim, H.-K.; Park, M.-J.; Hwang, D.-H.; Jung, B.-J. *Macromolecules* **2006**, *39*, 177. (b) Wong, K.-T.; Liao, Y.-L.; Lin, Y.-T.; Su, H.-C.; Wu. C.-c. *Org. Lett.* **2005**, *7*, 5131.

(22) (a) Finzi, C.; Fernandez, J. E.; Randazzo, M.; Toppare, L. *Macromolecules* **1992**, *25*, 245. (b) Murashima, T.; Hirai, K.; Une, Y.; Uchihara, Y.; Uno, H.; Ono, N. *Tetrahedron Lett.* **1998**, *39*, 5397.

(23) (a) Reynolds, J. R.; Katritzky, A. R.; Soloducho, J.; Belyakov, S.; Sotzing, G. A.; Pyo, M. *Macromolecules* **1994**, *27*, 7225. (b) Sotzing, G. A.; Reynolds, J. R.; Katritzky, A. R.; Soloducho, J.; Belyakov, S.;

Musgrave, R. *Macromolecules* **1996**, *29*, 1679. (c) Soloducho, J.; Roszak, S.; Chyla, A.; Tajchert, K. *New J. Chem.* **2001**, *25*, 1175.
(24) Kim, I. T.; Elsenbaumer, R. L. *Chem. Commun.* **1998**, 327.
(25) Roncali, J. *Chem. Rev.* **1997**, *97*, 173.
(26) (a) Eldo, J.; Arunkumar, E.; Ajayaghosh, A. *Tetrahedron Lett.* **2000**, *41*, 6241. (b) Büschel, M.; Ajayaghosh, A.; Eldo, J.; Daub, J. *Macromolecules* **2002**, *35*, 8405.
(27) (a) Ajayaghosh, A.; Eldo, J. *Org. Lett.* **2001**, *3*, 2595. (b) Eldo, J.; Ajayaghosh, A. *Chem. Mater.* **2002**, *14*, 410. (c) Ajayaghosh, A. *Chem. Soc. Rev.* **2003**, *32*, 181. (c) Ajayaghosh, A. *Acc. Chem. Res.* **2005**, *38*, 449.
(28) Wadsworth, W. S.; Emmons, W. D. *J. Am. Chem. Soc.* **1961**, *83*, 1733.
(29) (a) Agarawal, S.; Mohapatra, Y. N.; Singh, V. A.; Sharan, R. *J. Appl. Phys.* **1995**, *77*, 5725. (b) Biswas, A. K.; Tripathi, A.; Singh, S.; Mohapatra, Y. N. *Synth. Met.* **2005**, *155*, 340.
(30) (a) Agrawal, A. K.; Jenekhe, S. A. *Chem. Mater.* **1996**, *8*, 579. (b) de Leeuw, D. M.; Simenon, M. M. J.; Brown, A. R.; Einerhand, R. E. F. *Synth. Met.* **1997**, *87*, 53. (c) Chen, Z.-K.; Huang, W.; Wang, L.-H.; Kang, E.-T.; Chen, B. J.; Lee, C. S.; Lee, S. T. *Macromolecules* **2000**, *33*, 9015.

MA070116G